White Rose Research Online

eprints@whiterose.ac.uk
https://eprints.whiterose.ac.uk
Universities of Leeds, Sheffield and York

Deposited via The University of Sheffield.

White Rose Research Online URL for this paper:
https://eprints.whiterose.ac.uk/id/eprint/236795/

Version: Published Version

Article:
Zu, L., Giarè, W., Zhang, C. et al. (2026) A solution to the S8 tension through neutrino–dark matter interactions. Nature Astronomy. pp. 1-9. ISSN: 2397-3366

https://doi.org/10.1038/s41550-025-02733-1

Reuse
This article is distributed under the terms of the Creative Commons Attribution (CC BY) licence. This licence allows you to distribute, remix, tweak, and build upon the work, even commercially, as long as you credit the authors for the original work. More information and the full terms of the licence here:
https://creativecommons.org/licenses/

Takedown
If you consider content in White Rose Research Online to be in breach of UK law, please notify us by emailing eprints@whiterose.ac.uk including the URL of the record and the reason for the withdrawal request.

UNIVERSITY OF LEEDS
University of Sheffield
UNIVERSITY of York

nature astronomy

Article

https://doi.org/10.1038/s41550-025-02733-1

A solution to the S_8 tension through neutrino–dark matter interactions

Received: 26 February 2025

Accepted: 30 October 2025

Published online: 02 January 2026

Check for updates

Lei Zu [1], William Giarè [2], Chi Zhang [3,4,5], Eleonora Di Valentino [2], Yue-Lin Sming Tsai [3,4] & Sebastian Trojanowski [1,6]

Neutrinos and dark matter (DM) are two of the least understood components of the Universe, yet both play crucial roles in cosmic evolution. Clues about their fundamental properties may emerge from discrepancies in cosmological measurements across different epochs of cosmic history. Possible interactions between them could leave distinctive imprints on cosmological observables, offering a rare window into dark sector physics beyond the standard ΛCDM framework. Here we present compelling evidence that DM–neutrino interactions can resolve the persistent structure growth parameter discrepancy, $S_8 = \sigma_8\sqrt{\Omega_m/0.3}$, between early and late Universe observations. By incorporating cosmic shear measurements from current weak lensing surveys, we demonstrate that an interaction strength of $u \approx 10^{-4}$ not only provides a coherent explanation for the high-multipole observations from the Atacama Cosmology Telescope, but also alleviates the S_8 discrepancy. Combining early Universe constraints with DES Y3 cosmic shear data yields a nearly 3σ preference for non-zero DM–neutrino interactions. This strengthens previous observational claims and provides a clear path towards a breakthrough in cosmological research. Our findings challenge the standard ΛCDM paradigm and highlight the potential of future large-scale structure surveys, which can rigorously test this interaction and unveil the fundamental properties of DM.

Despite its established role in the Standard Cosmological Model (ΛCDM), the microscopic nature of dark matter (DM) remains unknown. It is assumed to be cold—that is, non-relativistic at decoupling—and to interact, at most, very weakly with baryonic matter[1–3]. Cosmology offers a powerful tool for probing the nature of DM, especially in the context of neutrino–DM interactions (νDM). Both the astrophysical and terrestrial searches for νDM interactions pose a challenge. These interactions can only be indirectly constrained by studying small deviations in neutrino properties from the Standard Model predictions due to new physics[4], or by searching for an excess in the astrophysical neutrino flux caused by DM annihilations in the Galactic centre[5].

Instead, in the early Universe, neutrinos contributed substantially to the radiation components, with a number density much higher than that of baryons. The νDM interactions induce diffusion-damped dark acoustic oscillations (DAO) in the matter power spectrum[6,7]. Therefore, such sizable couplings lead to deviations from the ΛCDM model, affecting the cosmic microwave background (CMB) radiation and large-scale structure (LSS) of the Universe. Consequently, cosmological observations are highly sensitive to νDM interactions[6–32].

Interestingly, recent analyses of CMB data have revealed a preference for non-zero νDM couplings, specifically in the high-multipole regime[22,23,27], which is consistent with earlier findings in the Lyman-α

[1]National Centre for Nuclear Research, Warsaw, Poland. [2]School of Mathematical and Physical Sciences, University of Sheffield, Sheffield, UK. [3]Key Laboratory of Dark Matter and Space Astronomy, Purple Mountain Observatory Chinese Academy of Sciences, Nanjing, China. [4]School of Astronomy and Space Science, University of Science and Technology of China, Hefei, China. [5]International School for Advanced Studies, SISSA, Trieste, Italy. [6]Astrocent, Nicolaus Copernicus Astronomical Center Polish Academy of Sciences, Warsaw, Poland. e-mail: Lei.Zu@ncbj.gov.pl; w.giare@sheffield.ac.uk; chizhang@pmo.ac.cn; e.divalentino@sheffield.ac.uk; smingtsai@pmo.ac.cn; Sebastian.Trojanowski@ncbj.gov.pl

flux power spectrum[20]. To further explore these interactions, we test νDM scenario predictions by incorporating weak lensing (WL) data, a low-redshift observation ($z < 3.5$), as a supplement to the high-redshift CMB data. Because the relative impact of νDM interactions grows at small scales, where nonlinear effects in structure formation become significant, we extend previous analyses by going beyond the linear evolution and including results of N-body simulations obtained on the basis of input matter power spectra modified in the presence of νDM interactions. To make such an analysis feasible, we follow a flexible approach introduced in ref. 33, which allows for the convenient reuse of results from previous simulations across various DAO scenarios and global parameter scans.

WL data are crucial for constraining cosmological parameters, especially for the S_8 amplitude defined as $S_8 = \sigma_8\sqrt{\Omega_m/0.3}$ (ref. 34), where σ_8 is the mass dispersion on a scale around $8h^{-1}$ Mpc and Ω_m is the total matter abundance. In the standard ΛCDM framework, the S_8 value derived from Planck CMB data is larger than the low-redshift measurements from WL surveys, leading to a 2–3σ tension[35–37]. In this work, we revisit this open question within the framework of the νDM model. By fitting the current 3-year Dark Energy Survey (DES) cosmic shear data alone[35], we identify a preferred region for non-zero νDM interaction strength. Intriguingly, this preferred region is consistent with that favoured by Atacama Cosmology Telescope (ACT) data. When combining all early- and late-Universe observational data, we find a nearly 3σ detection of the non-zero νDM interactions. We show that, for the preferred value of the νDM interaction strength, both the CMB and WL data lead to consistent fits of the S_8 parameter, therefore alleviating the persisting discrepancy.

To further explore the potential of next-generation observations, we generate mock cosmic shear data for upcoming surveys, including the Vera C. Rubin Observatory (formerly known as the Large Synoptic Survey Telescope, LSST)[38] and the China Space Station Telescope (CSST)[39]. Our results demonstrate that, with the improved sensitivity of these future surveys, the favoured interaction region will be either robustly confirmed or excluded.

The Article is organized as follows. In the Modelling νDM interactions section, we briefly discuss how νDM interactions are modelled in our study. The Results section is devoted to presenting the results of our study, and we conclude in the Discussion section. The Methods section discusses the implementation of the cosmological datasets in the analysis. Supplementary Information analyses the expected impact of νDM scatterings on the matter power spectrum beyond our main assumptions and presents our treatment of the WL data.

Modelling νDM interactions

In the linear regime of perturbation growth, the shape of the matter power spectrum is determined by solving the Boltzmann equation, which describes the phase-space evolution of the distribution function for various Standard Model species and DM, along with the coupled Einstein and fluid equations[40,41]. In the presence of νDM interactions, additional terms appear in the Boltzmann hierarchy, altering the evolution of perturbations. These interaction terms modify the energy transfer and momentum exchange between DM and neutrinos, leading to distinct imprints on the CMB anisotropies and the matter power spectrum, as detailed in refs. 11,42–44. The corresponding equations are readily solved for cold (non-relativistic) DM species after integrating over momentum. In particular, the equations describing the evolution of the density fluctuations δ_χ and the divergence of fluid velocity θ_χ are given by

$$\dot{\delta}_\chi = -\theta_\chi + 3\dot{\phi}, \tag{1}$$

$$\dot{\theta}_\chi = k^2\psi - \mathcal{H}\theta_\chi - K_\chi\dot{\mu}_\chi(\theta_\chi - \theta_\nu), \tag{2}$$

where ϕ and ψ are scalar potentials appearing in the line element of the perturbed flat Friedmann–Lemaître–Robertson–Walker Universe, and $\mathcal{H} = \dot{a}/a$ is the Hubble rate. We define $K_\chi = (1 + w_\nu)\rho_\nu/\rho_\chi$, where ρ_χ and ρ_ν are the DM and neutrino energy densities, respectively, and w_ν is the neutrino equation of state parameter. For massless neutrinos, one finds $w_\nu = 1/3$ and $K_\chi = (4/3)\rho_\nu/\rho_\chi$. From equation (2), the evolution of θ_χ is modified in the presence of the νDM interaction term, which is proportional to $\dot{\mu}_\chi$. In the massless neutrino case, this is given by $\dot{\mu}_\chi = a\, n_\chi \sigma_{\nu\mathrm{DM}}$, where the cold DM number density is $n_\chi = \rho_\chi/m_\chi$, the νDM scattering cross-section is denoted by $\sigma_{\nu\mathrm{DM}}$, and m_χ is the DM particle mass. Therefore, $K_\chi\dot{\mu}_\chi$ depends on the cross-section and the inverse of the DM mass. This dependence is commonly parameterized by the dimensionless quantity[11]

$$u_{\nu\mathrm{DM}} = \frac{\sigma_{\nu\mathrm{DM}}}{\sigma_\mathrm{T}}\left(\frac{m_\chi}{100\ \mathrm{GeV}}\right)^{-1}, \tag{3}$$

where σ_T is the Thomson scattering cross-section. The general expression for $\dot{\mu}_\chi$ is more complex for massive neutrinos, but the impact of the νDM interactions on perturbation evolution can still be effectively described by $u_{\nu\mathrm{DM}}$ in the cold DM regime. In this work, we consider the most thoroughly studied scenario, in which the neutrinos are massless, and the νDM interaction cross-section is independent of temperature. We refer to Supplementary Information for a discussion beyond this approximation and to the Methods section for details of our cosmological data analysis.

Results

Possible evidence of non-zero νDM interaction strength

As mentioned above, hints of non-negligible νDM interaction strength have been found in high-multipole ACT[22,23,27] and Lyman-α[20] data. For the purpose of this study, we have re-examined the CMB analysis including data from the Planck and ACT collaborations, and baryon acoustic oscillation (BAO) data (Planck+BAO+ACT likelihoods), by using the flat priors, shown in Supplementary Table 1. The relevant one-dimensional posterior distribution for $u_{\nu\mathrm{DM}}$ is shown as a solid black line in Fig. 1. We observe a preference for non-zero $u_{\nu\mathrm{DM}}$ within the 68% credible region, consistent with previous findings, which is driven by the high-ℓACT data. We note that our results for $u_{\nu\mathrm{DM}}$ are slightly shifted to higher values compared with previous works[27], as we used the full Plik likelihood with a cut at $\ell_{\max} = 650$ rather than the lite version. The preferred parameter regions are reported in Table 1, with a central value of $\log_{10} u_{\nu\mathrm{DM}} \approx -4.24$.

We now examine this anomaly using cosmic shear data. The posterior distribution obtained when fitting the DES Y3 cosmic shear likelihood only is shown with the dotted blue line in Fig. 1. In this case, we also find a mild preference towards non-zero $u_{\nu\mathrm{DM}}$, albeit with a lower statistical significance (<1σ). We discuss details of our cosmic shear analysis in the 'Weak lensing' section in Methods and further illustrate it in Supplementary Figs. 2 and 3. To test the interplay between the different datasets with regard to this anomaly, we next incorporate a combination of both early- and late-Universe observational data, Planck+BAO+ACT+DES Y3 cosmic shear. By using the combined dataset, we find robust evidence for a non-zero νDM interaction strength at nearly 3σ significance, with $u_{\nu\mathrm{DM}} \approx 10^{-4}$. This strengthens the preference found in the Planck+BAO+ACT and DES Y3 cosmic shear data. The corresponding posterior distribution for $u_{\nu\mathrm{DM}}$ is shown with the solid green line in Fig. 1, and the relevant parameter ranges are given in Table 1. The relevant χ^2 values and triangle posterior distributions of the model parameters are presented in Supplementary Table 2 and Supplementary Fig. 4.

For a complementary perspective, the right panel of Fig. 2 also shows the $\Delta\chi^2$ curves obtained from each case using the profile likelihood method. This demonstrates the robustness of the preferred parameter region under different statistical approaches. A detailed breakdown of the χ^2 values for each component is provided in Supplementary Table 1.

This result suggests that the νDM interaction with $u_{\nu\mathrm{DM}} \approx 10^{-4}$ is consistently supported by both CMB and WL cosmological data,

https://doi.org/10.1038/s41550-025-02733-1

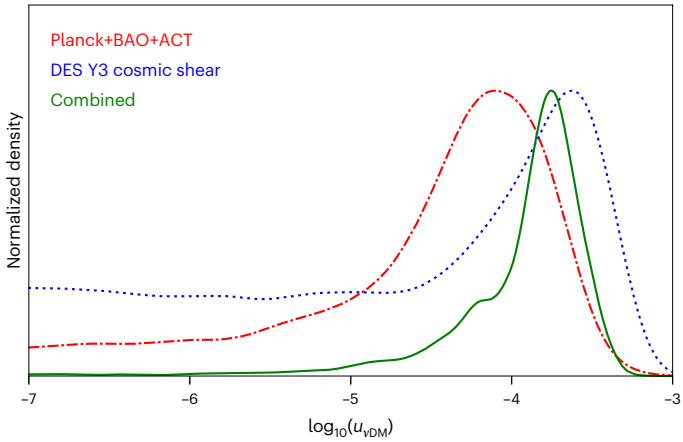

Fig. 1 | Posterior distributions of the DM–neutrino interaction parameter $u_{\nu DM}$. The dash-dotted red (dotted blue) line represents the results obtained using the Planck+BAO+ACT (DES Y3 cosmic shear) likelihood. The combined results for the likelihood Planck+BAO+ACT+DES Y3 cosmic shear are presented as a solid green line.

Table 1 | The 68% credible intervals for the cosmological parameters

Parameter	Planck+BAO+ACT	+DES Y3 cosmic shear
$100\Omega_b h^2$	$2.235^{+0.014}_{-0.014}$	$2.247^{+0.014}_{-0.014}$
Ω_m	$0.3060^{+0.0060}_{-0.0060}$	$0.2983^{+0.0048}_{-0.0048}$
$100\theta_s$	$1.04218^{+0.00034}_{-0.00049}$	$1.04225^{+0.00047}_{-0.00028}$
$\ln(10^{10}A_s)$	$3.036^{+0.015}_{-0.015}$	$3.029^{+0.016}_{-0.013}$
n_s	$0.9728^{+0.0047}_{-0.0047}$	$0.9742^{+0.0046}_{-0.0046}$
τ_{reio}	$0.0487^{+0.0069}_{-0.0081}$	$0.0484^{+0.0088}_{-0.0070}$
$\log_{10} u_{\nu DM}$	$-4.24^{+0.56}_{-0.71}$	$-3.70^{+0.21}_{-0.34}$
S_8	$0.811^{+0.024}_{-0.017}$	$0.766^{+0.024}_{-0.020}$

The 68% credible regions for the cosmological parameters, obtained using the Planck+BAO+ACT and Planck+BAO+ACT+DES Y3 cosmic shear likelihoods.

despite these being independent observational probes spanning different epochs in cosmic history. This convergence highlights the potential of νDM interactions as a compelling extension beyond the standard ΛCDM paradigm, offering new insights into the fundamental nature of DM and its role in cosmic evolution.

It is important to note that interpreting the observed preference in terms of a constant $u_{\nu DM}$ parameter could face challenges from small-scale observations, such as the Lyman-α forest[20], dwarf galaxy counts[28] and galaxy luminosity functions[45]. We note, however, that these small-scale probes are subject to considerable astrophysical uncertainties, particularly those arising from baryonic feedback processes. Such effects can alter the interpretation of structure formation and may introduce non-negligible, model-dependent systematics into the derived constraints on νDM interactions.

More importantly, the cosmological observables used in our analysis—the CMB and cosmic shear—probe perturbations at different scales and epochs compared with those examined by the Lyman-α forest or galaxy luminosity functions. This apparent tension could be alleviated if the νDM interaction is not constant but instead varies with redshift, for example, through an energy-dependent scattering cross-section as motivated by specific particle physics models[46]. Therefore, the working assumption of a constant νDM cross-section applied in our study should be considered a useful and widely adopted phenomenological approximation. It allows us to capture the essential preferences in the considered datasets, while acknowledging that further investigations into specific νDM model implementations are warranted.

S_8 discrepancy

As mentioned in the main text, suppression of perturbations at scales probed by WL surveys has an important effect on the matter clustering parameter $S_8 = \sigma_8\sqrt{\Omega_m/0.3}$. It has been shown that the persisting tension between the CMB and WL estimates of this parameter, known as the S_8 discrepancy (cf. refs. 47–49 for review), can be alleviated by νDM interactions[15]. We revisit this possibility by consistently including the entire Planck+BAO+ACT+DES Y3 cosmic shear dataset in the analysis.

The results of the marginalized two-dimensional (2D) posterior distribution in the (S_8, $u_{\nu DM}$) plane are presented in the left panel of Fig. 2. In the plot, we present the results obtained separately for Planck+BAO+ACT and DES Y3 cosmic shear data and the combined analysis. As can be seen, for small values of $u_{\nu DM} < 10^{-6}$, the impact of νDM interactions is negligible at perturbation scales characteristic to S_8. In this case, the ΛCDM regime is effectively recovered for both the CMB and WL data, and the 2σ regions obtained for the early and late Universe datasets show no overlap. Hence, the S_8 discrepancy persists, as expected.

However, for larger values of $u_{\nu DM}$, the data are consistent with lower values of S_8, leading to a better agreement between CMB and WL observations. When combining datasets (Planck+BAO+ACT+DES Y3 cosmic shear), we resolve the S_8 tension, as shown with green-shaded regions in the plot. Remarkably, the value of the νDM interaction strength required for this, $u_{\nu DM} \approx 10^{-4}$, corresponds to the previously reported 3σ evidence found in the combined dataset (cf. also Table 1).

Future prospects

The above results highlight the potential of νDM interactions to address persisting discrepancies in cosmological data that will be decisively studied in next-generation cosmological surveys. To investigate the relevant prospects of future WL observations, we additionally perform Markov Chain Monte Carlo (MCMC) scans, combining the mock data with the Planck+BAO+CSST and Planck+BAO+LSST likelihoods. The resulting likelihood profiles, shown in Fig. 3 (light-green and grey lines), indicate that these future WL surveys have the potential to constrain the νDM interaction parameter to $\log_{10} u_{\nu DM} \lesssim -5.3$ (CSST) or even $\log_{10} u_{\nu DM} \lesssim -5.9$ (LSST) at 95% confidence level, assuming the peak we observe is a spurious result and the true cosmology is ΛCDM, that is, DM is effectively not interacting with neutrinos at redshifts relevant to our analysis. As can be seen, a substantial improvement in sensitivity is expected from these next-generation WL surveys. In particular, the preferred parameter region obtained by fitting ACT and DES Y3 cosmic shear data, as indicated with an orange shading in the plot, will be either thoroughly confirmed or excluded by these surveys. When using mock data generated from a νDM interacting scenario, the 1σ error bar on $\log_{10} u_{\nu DM}$ is reduced from ±0.55 (DES) to ±0.08 (CSST), demonstrating the promising discovery potential of upcoming WL surveys.

Discussion

Cosmological surveys and gravitational lensing observations provide compelling evidence for the existence of DM, but they may also offer critical insights into its fundamental nature. Probing possible interactions of DM with neutrinos remains particularly challenging in terrestrial searches (see refs. 50,51 for reviews), although this challenge can be mitigated by studying the impact of νDM scatterings on the matter power spectrum in the early Universe. Recent studies have uncovered a slight preference for non-negligible νDM interactions in high-multipole CMB data and Lyman-α forest observations.

https://doi.org/10.1038/s41550-025-02733-1

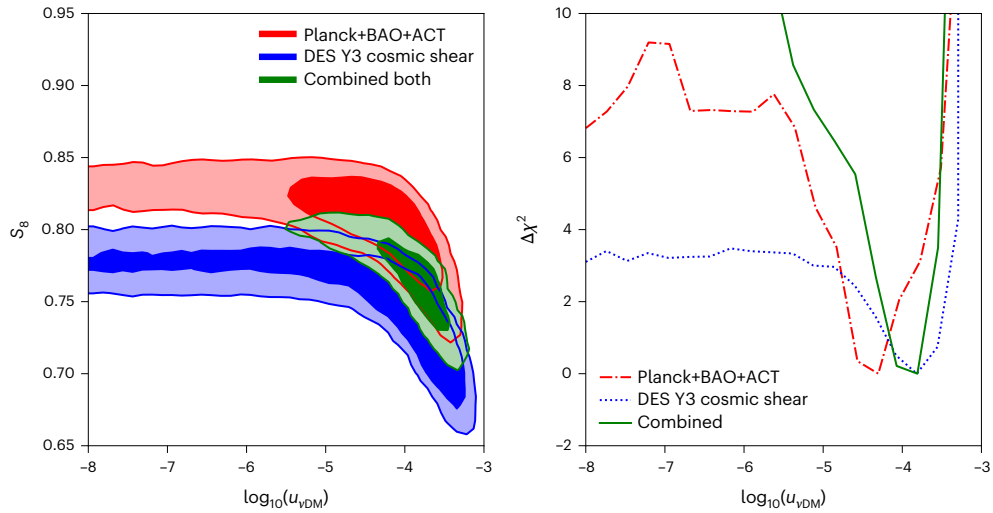

Fig. 2 | Profile likelihood distribution and marginalized 2D posterior distribution in the (S_8, $u_{\nu DM}$) plane. Left: marginalized 2D posterior distribution in the (S_8, $u_{\nu DM}$) plane. The red and blue contours show the results for the Planck+BAO+ACT and DES Y3 cosmic shear datasets, respectively. The green region represents the results for the combined Planck+BAO+ACT+DES Y3 cosmic shear dataset. Right: the $\Delta\chi^2$ with the parameter $u_{\nu DM}$ obtained using the profile likelihood method from the analysis of Planck+BAO+ACT, DES Y3 cosmic shear and combined datasets.

In this study, we utilized WL surveys to investigate νDM interactions further. We computed the matter power spectrum incorporating nonlinear corrections from *N*-body simulations. These simulations evolve perturbations solely through gravity, as the νDM interactions are expected to decouple at early times and do not affect matter distributions at the scales probed in our study. We used an emulator that interpolates matter power spectra from predefined simulations to apply *N*-body results in cosmological parameter scans.

DES Y3 cosmic shear data alone, which are free from galaxy bias, reveal a preference for non-zero DM–neutrino interaction strength. This preference endures even when combining WL data with CMB and BAO datasets. We find that the Planck+BAO+ACT+DES Y3 cosmic shear data favour non-zero $u_{\nu DM}$ at nearly the 3σ level. This preferred interaction strength, $u_{\nu DM} \approx 10^{-4}$, can also simultaneously alleviate the persistent S_8 tension. The preference for non-zero $u_{\nu DM}$ in the data is additionally linked to a broadening of the Ω_m distribution, as shown in Supplementary Fig. 4. While the νDM scenario permits a larger value for this parameter, the amount of structures does not increase proportionally. This leads to an overall improved cosmological fit.

Although the statistical significance of these anomalies is not yet sufficient to definitively rule out the standard cosmological scenario, the discrepancies across different observables and datasets underscore the importance of further investigation. Future high-precision WL surveys are expected to provide deeper insights into the mass distribution, particularly at small scales, enabling more stringent tests of νDM interactions—especially in parameter regions suggested by ACT and DES Y3 cosmic shear observations.

The suppression in the matter power spectrum favoured by our analysis could potentially arise in other well-motivated extensions of the ΛCDM model, beyond νDM interactions. These include DM interactions with baryons[52], photons[53] or dark radiation[54], as well as models with warm DM[55] or ultralight (fuzzy) DM[56]. While these models can produce qualitatively similar effects on the linear matter power spectrum, νDM interactions offer distinct advantages. First, this scenario is less constrained by CMB observations compared with DM interactions with other Standard Model species. Second, unlike warm DM or fuzzy DM—where the suppression scale is typically fixed by the DM particle mass—the νDM interaction can exhibit redshift dependence or affect only a fraction of the DM, providing greater flexibility to avoid small-scale bounds (cf. discussion in Supplementary Information). While νDM interactions offer a particularly compelling explanation for the observed deviations, which can also be independently tested in future terrestrial searches, other beyond-ΛCDM models predicting scale-dependent suppression of the power spectrum could provide alternative explanations that should likewise be tested (cf., for example, refs. 57,58). The standard cosmological model is under growing pressure, but new hints in cosmological data are driving us towards finding a valid extension.

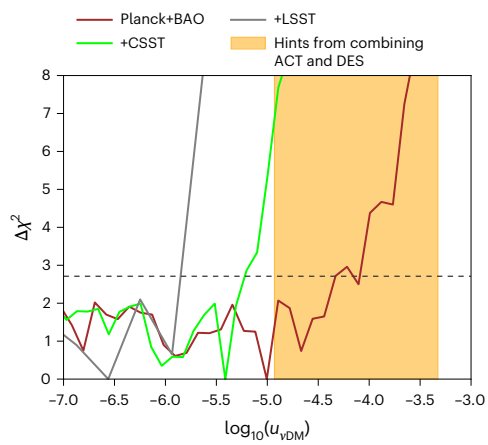

Fig. 3 | Forecasted constraints on the DM–neutrino interaction strength from future WL surveys. Variation of $\Delta\chi^2$ with the parameter $u_{\nu DM}$ obtained using the profile likelihood method[92]. The brown line represents the Planck+BAO likelihood, while the light-green and grey lines additionally include mock cosmic shear data from CSST and LSST, respectively. The dashed black line indicates $\Delta\chi^2 = 2.71$, corresponding to the 2σ upper limit. The orange-shaded region indicates the 95% confidence level preferred range of the $u_{\nu DM}$ parameter found in the Planck+BAO+ACT+DES Y3 cosmic shear data.

Note added

After the submission of this Article, the KiDS-Legacy survey reported a higher value for the structure growth parameter, $S_8 = 0.815^{+0.016}_{-0.021}$, which is in good agreement with the Planck ΛCDM prediction. As these data are not yet publicly available, we cannot assess their impact on our results. However, we stress that the preference we find in our data is not driven by the global S_8 tension. Our constraints are primarily informed by cosmic shear measurements sensitive to both

quasi-nonlinear scales around ($k \approx 1h$ Mpc^{-1}) and the S_8 more linear scales (for example, ($k \lesssim 0.7h$ Mpc^{-1})). We do expect that, if larger values of S_8 are consistently favoured by the new data and other WL surveys in the future, then smaller—yet non-vanishing—values of $u_{\nu\mathrm{DM}}$ might be preferred in the fit, in line with previous findings based on CMB data alone[22,23,27] and Lyman-α observations[20]. A status review of this discrepancy can be found in ref. 59.

Methods

Cosmological data analysis

We use a modified version of the CLASS code to model the evolution of the Universe, specifically accounting for νDM interactions[43,44]. In our analysis, we vary $u_{\nu\mathrm{DM}}$. We also include the six ΛCDM parameters: the baryon Ω_b and DM Ω_DM energy densities (assuming all of DM interacts with neutrinos), the amplitude A_s and spectral index n_s of primordial scalar perturbations, the optical depth to reionization τ_reio, and the angular size of the horizon at the last scattering surface θ. The prior ranges of each parameters are presented in Supplementary Table 1. We have verified that using a flat linear prior on the parameter $u_{\nu\mathrm{DM}}$ does not alter our main conclusions. The effective number of relativistic degrees of freedom is fixed to $\Delta N_\mathrm{eff} = 3.044$. The following cosmological data are included in the likelihood:

(1) The DES 3-year cosmic shear likelihood[35]. We build an emulator to model the nonlinear correction to the matter power spectrum, calibrated on 200 N-body simulations generated with DAO-modified initial conditions.The linear matter power spectrum is first computed using the modified CLASS code, and the emulator is then used to obtain its nonlinear counterpart (cf. ref. 33 for further details). The resulting nonlinear power spectrum is used to predict the cosmic shear signal for a given intrinsic-alignment model (see 'Weak lensing' section for more details). We refer to this dataset as DES Y3 cosmic shear throughout this work. We account for nonlinear effects of the gravitational potential on the matter power spectrum at small scales, $k \gtrsim 1h$ Mpc^{-1} using N-body simulations. Notably, on top of the cosmic shear data, the DES Y3 dataset contains galaxy clustering and galaxy–galaxy lensing data. These are, however, subject to unknown galaxy bias, which describes the bias arising from using galaxies as tracers of matter[36,60]. In this Article, we focus on the most robust conclusions based solely on cosmic shear. Further details on the analysis of the DES Y3 dataset and the implementation of nonlinear effects in the matter power spectrum are given in the 'Weak lensing' section.

(2) The CMB likelihoods from Planck 2018 Legacy (P18)[61], including high-ℓ power spectra (TT, TE and EE), low-ℓ power spectra (TT and EE) and the Planck lensing reconstruction. The official Planck likelihoods are used directly, and their implementation is interfaced through Montepython. We refer to this dataset as Planck.

(3) We use the BOSS DR12 BAO likelihood, which combines distance measurements at $z = 0.106$, 0.15 and 0.2–0.75 (refs. 62–64), referred to as BAO. The likelihood is implemented following the public SDSS likelihood module, assuming Gaussian priors on the measured distance ratios.
For comparison, we also included the new BAO likelihood incorporating the BOSS DR16 dataset[65–69] in the data analysis. Including the updated BAO dataset yields nearly identical bounds on $u_{\nu\mathrm{DM}}$ as those obtained with DR12, demonstrating the robustness of our results to this update.

(4) The full ACT temperature and polarization DR4 likelihood[70]. We use HMCode[71] for nonlinear correction to the matter power spectrum. We have verified that the angular power spectra obtained from HMCode are consistent with those from our emulator at percent level. We refer to this dataset as ACT.
When combining the Planck and ACT datasets, we applied a conservative cut of $\ell < 650$ on the Planck data to avoid double-counting in the overlapping multipole range. In this way, the combined dataset utilizes the large-scale information from Planck and the small-scale measurements from ACT. We have additionally confirmed with a sample scan that including the ACT CMB lensing DR6 likelihood[72–74] does not alter our results. The ACT DR6 lensing data were cut at $\ell < 800$ for this purpose.

(5) To further investigate the potential of future WL observations, we utilize the expected sensitivity of the upcoming CSST and LSST cosmic shear surveys. Using the publicly available code CosmoCov[75,76], we compute the covariance matrix to represent cosmic shear sensitivity, incorporating the CSST and LSST window functions. The fiducial model we used for these forecasts is the ΛCDM with Planck cosmological parameters.

Weak lensing

Weak gravitational lensing enables the direct mapping of the late-time LSS of the Universe by statistically analysing the shape distortions of numerous galaxies induced by foreground matter fields. The comprehensive set of WL measurements, known as 3 × 2pt, consists of three two-point correlation functions with angular separation θ of galaxy pairs: galaxy clustering $w(\theta)$ (position–position), galaxy–galaxy lensing $\gamma_\mathrm{t}(\theta)$ (position–shape) and cosmic shear $\xi_\pm(\theta)$ (shape–shape). The quantity $w(\theta)$ measures the angular clustering of foreground lens galaxies, while $\gamma_\mathrm{t}(\theta)$ measures the correlation between the positions of foreground lens galaxies and the shape distortions of background source galaxies at an angular separation θ. Finally, $\xi_\pm(\theta)$ measures cosmic shear, that is, the correlation between the shape distortions of background source galaxies due to the foreground LSS. Compared with the galaxy–galaxy lensing and galaxy clustering, the cosmic shear is independent of the galaxy bias, which describes the bias arising from using galaxies as tracers of matter[36,60].

Therefore, the analyses based solely on cosmic shear data lead to the most robust conclusions that we present in the following. When analysing cosmic shear data, nonlinear effects of the gravitational potential play an important role in the evolution of LSS at small scales, $k \gtrsim 1h$ Mpc^{-1}. We account for these nonlinear effects using N-body simulations.

***N*-body simulation.** As discussed above, νDM interactions primarily affect WL data through DAO, which modify the initial matter power spectrum used in N-body simulations. Following ref. 33 (cf. equations (3.1) and (3.2) therein), we use the modified Boltzmann code CLASS[44] to compute the ratio of linear matter power spectra between ΛCDM and the νDM scenario. While this ratio depends on k, we effectively reduce its dimensionality to two parameters using principal component analysis[77]. This allows us to construct a two-parameter grid mapping linear to nonlinear matter power spectra, based on 205 N-body simulations run with the GIZMO code[78,79]. These simulations were initialized with different matter power spectra corresponding to the interacting DM model. For arbitrary values of $u_{\nu\mathrm{DM}}$, we map the corresponding linear power spectrum ratio onto this grid and deduce the nonlinear result through interpolation. Finally, we obtain the nonlinear matter power spectrum for the νDM scenario by multiplying this nonlinear ratio with the nonlinear ΛCDM power spectrum from Halofit[80].

Although the original map of nonlinear power spectrum ratios in ref. 33 used DM–baryon interactions, a similar procedure applies to the νDM case. This is because the parameterization of the linear matter power spectrum ratios via principal component analysis is the same, and the N-body simulations evolve solely through gravity. To verify this, we performed an N-body simulation for the νDM scenario with $\log_{10} u_{\nu\mathrm{DM}} = -4.6$ and compared the resulting nonlinear matter power spectrum with that obtained from the emulator (that is, by

interpolating on the grid). The comparison is shown in the left panel of Supplementary Fig. 2. This plot has been obtained by neglecting the impact of Halofit. We also present the uncertainty of the simulation in the plot. Because our simulations are performed within a finite comoving volume, the large-scale density fluctuations on scales comparable to or larger than the box size are dominated by the cosmic variance. The relative uncertainty scales approximately as $\Delta P/P \sim 1/\sqrt{N_{\rm modes}} \approx 1/L_{\rm box}^{3/2}$, highlighting that a larger box volume is required to reduce this large-scale variance, where $N_{\rm modes}$ is the number of independent Fourier modes available in a bin centred at wavenumber k and $L_{\rm box}$ is the box size $200h^{-1}$ Mpc. The two results agree well, matching within nearly 15% uncertainty for $k \approx 1h$ Mpc^{-1}.

We also show the uncertainty in $\Delta P(k) = P_{N\text{-body}}(k) - P_{\rm em}(k)$ in the right panel of Supplementary Fig. 2. These results were obtained for the best-fit point in our analysis and for a similar scenario with the same cosmological parameters, except for a lower νDM interaction strength of $u_{\nu\rm DM} = 10^{-5}$. As can be seen, both results correspond to qualitatively distinct behaviours. This indicates a lack of systematic bias in the emulator results.

To quantify the impact of these differences, we computed the corresponding χ^2 values using the DES Y3 cosmic shear likelihood. For the best-fit point, we found $\chi^2_{\rm emu} = 240.6$ and $\chi^2_{N\text{-body}} = 239.1$ for the most compatible N-body simulation result within the uncertainty bars. This difference of $\Delta\chi^2 \approx 1.5$ is well within the statistical uncertainties of the dataset and smaller than the discrepancy introduced by using more approximate nonlinear tools, such as $\chi^2_{\rm HMCode} = 399.8$ and $\chi^2_{\rm Halofit} = 8{,}246.6$. Therefore, while the emulator does introduce a modelling uncertainty, it provides a substantially more accurate and reliable nonlinear correction compared with HMCode or Halofit, while maintaining the flexibility needed for MCMC scans.

We note, however, that a stronger bias might be introduced by using the Halofit nonlinear power spectrum (obtained on the basis of Gadget-2), when accounting for the impact of variations in other cosmological parameters, as discussed above and in ref. 33. In particular, for the specific points in the parameter space tested in Supplementary Fig. 2, we have found a systematic bias between GIZMO and Halofit results of order $\mathcal{O}(10\%)$ for $k \approx 0.1$–$1h$ Mpc^{-1}. This may impact the precise value of the best-fit point $u_{\nu\rm DM}$ parameter obtained in the MCMC scan in our analysis, as it appears slightly sensitive to the choice of the baseline simulation results (the difference between $\log u_{\nu\rm DM} = -3.7$ and -4.0 obtained in additional tests).

WL data. We use the current DES Y3 cosmic shear data in our analysis. This dataset contains the shapes of over 10^8 source galaxies across an effective area of 4,143 deg^2. The shape catalogue METACALIBRATION used in the DES Y3 analysis is divided into four redshift bins in the redshift range of $0 < z < 3$ (ref. 35). Following ref. 35, we mask small angular scales to reduce uncertainties from baryonic effects. We also utilize cosmic shear mock data from CSST and LSST for future forecasts. The redshift distributions for CSST and DES are different; thus, the CSST mask may not precisely reflect real conditions. However, the capabilities of the future telescope to detect distant galaxies make this mask a conservative estimate. For LSST, we present results with the masking scale set at $l < l_{\rm max} = 3{,}000$ following refs. 81,82.

Supplementary Fig. 3 shows the impact of νDM interactions on the cosmic shear signal. It illustrates the deviation in the expected cosmic shear signal (4th–4th bin) for two selected values of the νDM interaction strength, $\log_{10}(u_{\nu\rm DM}) = -4.6$ and -3.3, along with the DES Y3 data points. Nonlinear corrections are applied, as previously described. Stronger interactions lead to greater suppression of the matter power spectrum, which determines the shape of the blue and red curves. For comparison, the linear results are also shown with dotted lines. The nonlinear effects are significant, enhancing the signal at small angular scales. This effect is opposite to that of νDM interactions; the signal enhancement due to nonlinear effects is partially offset by increasing $u_{\nu\rm DM}$.

By treating neutrinos as massless in our analysis, we neglect the impact of their gravitational potential in the N-body simulations. We stress that, for a total neutrino mass $\sum m_\nu = 0.06$ eV, the resulting suppression of the nonlinear matter power spectrum is expected to be less than 5% at $k \approx 1h$ Mpc^{-1} (ref. 83). This effect is smaller than the uncertainty introduced by our emulator.

It is worth noting that increasing the neutrino mass beyond this limit can impact the matter power spectrum, particularly at late times and on small scales, and could even affect the inferred value of S_8 (ref. 84). Moreover, because $\sum m_\nu$ is negatively correlated with H_0 (refs. 85,86), its inclusion could shift the preferred H_0 value downwards, potentially exacerbating the H_0 tension. However, because the cosmological upper bound on the neutrino mass is primarily driven by BAO data—and these constraints are becoming increasingly stringent[68,87–89] (if not favouring a negative mass[90,91])—we adopt a massless neutrino approximation for simplicity.

While our main results are derived from cosmic shear data, we also analysed the full DES Y3 3 × 2pt dataset for completeness. This analysis also indicates a preference for a non-vanishing $u_{\nu\rm DM}$, although the statistical significance is reduced from nearly 3σ to below 2σ. In this case, the peak of the posterior distribution for the neutrino interaction parameter is also shifted, favouring a lower interaction strength of $\log_{10} u_{\nu\rm DM} = -4.60^{+0.55}_{-3.17}$. We attribute this discrepancy to the limitations of applying a ΛCDM-based galaxy bias model within our interacting dark sector scenario. Therefore, a more robust and model-compatible treatment of galaxy bias is necessary to draw stronger conclusions from the full 3 × 2pt dataset.

Data availability

The data used in this study are publicly available from the corresponding survey archives. The Planck 2018 Legacy Release data can be accessed via the ESA Planck Legacy Archive at https://www.cosmos.esa.int/web/planck/pla. The DES Y3 WL and shear catalogues are available from the DES Data Release Portal: the shape catalogues at https://des.ncsa.illinois.edu/releases/y3a2/Y3key-catalogs and the cosmic shear data products at https://des.ncsa.illinois.edu/releases/y3a2/Y3key-products. The ACT DR4 temperature and polarization power spectra are provided via the NASA LAMBDA archive at https://lambda.gsfc.nasa.gov/product/act/act_dr4_maps_info.html. The BAO measurements are taken from the BOSS DR12 and eBOSS DR16 galaxy catalogues, accessible via the SDSS Science Archive Server at https://www.sdss4.org/science/final-bao-and-rsd-measurements-table/.

References

1. Roszkowski, L., Sessolo, E. M. & Trojanowski, S. WIMP dark matter candidates and searches—current status and future prospects. *Rept. Prog. Phys.* **81**, 066201 (2018).
2. Boveia, A. et al. Snowmass 2021 Dark Matter Complementarity Report. Preprint at https://arxiv.org/abs/2211.07027 (2022).
3. Arcadi, G. et al. The waning of the WIMP: endgame? *Eur. Phys. J. C* **85**, 152 (2025).
4. Sajjad Athar, M. et al. Status and perspectives of neutrino physics. *Prog. Part. Nucl. Phys.* **124**, 103947 (2022).
5. Argüelles, C. A. et al. Dark matter annihilation to neutrinos. *Rev. Mod. Phys.* **93**, 035007 (2021).
6. Mangano, G., Melchiorri, A., Serra, P., Cooray, A. & Kamionkowski, M. Cosmological bounds on dark matter–neutrino interactions. *Phys. Rev. D* **74**, 043517 (2006).
7. Serra, P., Zalamea, F., Cooray, A., Mangano, G. & Melchiorri, A. Constraints on neutrino–dark matter interactions from cosmic microwave background and large scale structure data. *Phys. Rev. D* **81**, 043507 (2010).
8. Boehm, C., Fayet, P. & Schaeffer, R. Constraining dark matter candidates from structure formation. *Phys. Lett. B* **518**, 8–14 (2001).

9. Boehm, C. & Schaeffer, R. Constraints on dark matter interactions from structure formation: damping lengths. *Astron. Astrophys.* **438**, 419–442 (2005).
10. Shoemaker, I. M. Constraints on dark matter protohalos in effective theories and neutrinophilic dark matter. *Phys. Dark Univ.* **2**, 157–162 (2013).
11. Wilkinson, R. J., Boehm, C. & Lesgourgues, J. Constraining dark matter–neutrino interactions using the CMB and large-scale structure. *J. Cosmol. Astropart. Phys.* **05**, 011 (2014).
12. Boehm, C., Schewtschenko, J. A., Wilkinson, R. J., Baugh, C. M. & Pascoli, S. Using the Milky Way satellites to study interactions between cold dark matter and radiation. *Mon. Not. R. Astron. Soc.* **445**, L31–L35 (2014).
13. Bertoni, B., Ipek, S., McKeen, D. & Nelson, A. E. Constraints and consequences of reducing small scale structure via large dark matter-neutrino interactions. *J. High. Energy Phys.* **04**, 170 (2015).
14. Escudero, M., Mena, O., Vincent, A. C., Wilkinson, R. J. & Bœhm, C. Exploring dark matter microphysics with galaxy surveys. *J. Cosmol. Astropart. Phys.* **09**, 034 (2015).
15. Di Valentino, E., Bøehm, C., Hivon, E. & Bouchet, F. R. Reducing the H_0 and σ_8 tensions with dark matter–neutrino interactions. *Phys. Rev. D* **97**, 043513 (2018).
16. Olivares-Del Campo, A., Bœhm, C., Palomares-Ruiz, S. & Pascoli, S. Dark matter–neutrino interactions through the lens of their cosmological implications. *Phys. Rev. D* **97**, 075039 (2018).
17. Escudero, M., Lopez-Honorez, L., Mena, O., Palomares-Ruiz, S. & Villanueva-Domingo, P. A fresh look into the interacting dark matter scenario. *J. Cosmol. Astropart. Phys.* **06**, 007 (2018).
18. Becker, N., Hooper, D. C., Kahlhoefer, F., Lesgourgues, J. & Schöneberg, N. Cosmological constraints on multi-interacting dark matter. *J. Cosmol. Astropart. Phys.* **02**, 019 (2021).
19. Paul, A., Chatterjee, A., Ghoshal, A. & Pal, S. Shedding light on dark matter and neutrino interactions from cosmology. *J. Cosmol. Astropart. Phys.* **10**, 017 (2021).
20. Hooper, D. C. & Lucca, M. Hints of dark matter–neutrino interactions in Lyman-α data. *Phys. Rev. D* **105**, 103504 (2022).
21. Dey, A., Paul, A. & Pal, S. Constraints on dark matter–neutrino interaction from 21-cm cosmology and forecasts on SKA1-Low. *Mon. Not. R. Astron. Soc.* **524**, 100–107 (2023).
22. Brax, P., van de Bruck, C., Di Valentino, E., Giarè, W. & Trojanowski, S. New insights on *ν*–DM interactions. *Mon. Not. R. Astron. Soc.* **527**, L122–L126 (2023).
23. Brax, P., van de Bruck, C., Di Valentino, E., Giarè, W. & Trojanowski, S. Extended analysis of neutrino–dark matter interactions with small-scale CMB experiments. *Phys. Dark Univ.* **42**, 101321 (2023).
24. Akita, K. & Ando, S. Constraints on dark matter-neutrino scattering from the Milky-Way satellites and subhalo modeling for dark acoustic oscillations. *J. Cosmol. Astropart. Phys.* **11**, 037 (2023).
25. Pal, S., Samanta, R. & Pal, S. Revisiting coupled CDM-massive neutrino perturbations in diverse cosmological backgrounds. *J. Cosmol. Astropart. Phys.* **12**, 004 (2023).
26. Dey, A., Paul, A. & Pal, S. Imprints of dark matter–massive neutrino interaction in upcoming post-reionization and galaxy surveys. *Mon. Not. R. Astron. Soc.* **527**, 790–802 (2023).
27. Giarè, W., Gómez-Valent, A., Di Valentino, E. & van de Bruck, C. Hints of neutrino dark matter scattering in the CMB? Constraints from the marginalized and profile distributions. *Phys. Rev. D* **109**, 063516 (2024).
28. Crumrine, W., Nadler, E. O., An, R. & Gluscevic, V. Dark matter coupled to radiation: limits from the Milky Way satellites. *Phys. Rev. D* **111**, 023530 (2025).
29. Mosbech, M. R. et al. DESI forecast for dark matter–neutrino interactions using EFTofLSS. *J. Cosmol. Astropart. Phys.* **05**, 040 (2025).
30. Green, D., Kaplan, D. E. & Rajendran, S. Neutrino interactions in the late Universe. *J. High Energy Phys.* **11**, 162 (2021).
31. Mosbech, M. R., Boehm, C. & Wong, Y. Y. Y. Probing dark matter interactions with 21cm observations. *J. Cosmol. Astropart. Phys.* **03**, 047 (2023).
32. Loverde, M. & Weiner, Z. J. Probing neutrino interactions and dark radiation with gravitational waves. *J. Cosmol. Astropart. Phys.* **02**, 064 (2023).
33. Zhang, C., Zu, L., Chen, H.-Z., Tsai, Y.-L. S. & Fan, Y.-Z. Weak lensing constraints on dark matter–baryon interactions with N-body simulations and machine learning. *J. Cosmol. Astropart. Phys.* **08**, 003 (2024).
34. Abbott, T. M. C. et al. Dark Energy Survey year 1 results: cosmological constraints from galaxy clustering and weak lensing. *Phys. Rev. D* **98**, 043526 (2018).
35. Amon, A. et al. Dark Energy Survey Year 3 results: cosmology from cosmic shear and robustness to data calibration. *Phys. Rev. D* **105**, 023514 (2022).
36. Abbott, T. M. C. et al. Dark Energy Survey Year 3 results: cosmological constraints from galaxy clustering and weak lensing. *Phys. Rev. D* **105**, 023520 (2022).
37. Asgari, M. et al. KiDS-1000 Cosmology: cosmic shear constraints and comparison between two point statistics. *Astron. Astrophys.* **645**, A104 (2021).
38. Abell, P. A. et al. LSST Science Book, version 2.0. Preprint at https://arxiv.org/abs/0912.0201 (2009).
39. Gong, Y. et al. Cosmology from the Chinese Space Station Optical Survey (CSS-OS). *Astrophys. J.* **883**, 203 (2019).
40. Kodama, H. & Sasaki, M. Cosmological perturbation theory. *Prog. Theor. Phys. Suppl.* **78**, 1–166 (1984).
41. Ma, C.-P. & Bertschinger, E. Cosmological perturbation theory in the synchronous and conformal Newtonian gauges. *Astrophys. J.* **455**, 7–25 (1995).
42. Oldengott, I. M., Rampf, C. & Wong, Y. Y. Y. Boltzmann hierarchy for interacting neutrinos I: formalism. *J. Cosmol. Astropart. Phys.* **04**, 016 (2015).
43. Stadler, J., Bœhm, C. & Mena, O. Comprehensive study of neutrino–dark matter mixed damping. *J. Cosmol. Astropart. Phys.* **08**, 014 (2019).
44. Mosbech, M. R. et al. The full Boltzmann hierarchy for dark matter–massive neutrino interactions. *J. Cosmol. Astropart. Phys.* **03**, 066 (2021).
45. Mosbech, M. R. et al. Gravitational-wave event rates as a new probe for dark matter microphysics. *Phys. Rev. D* **108**, 043512 (2023).
46. Trojanowski, S. & Zu, L. Cosmological impact of *ν*DM interactions enhanced in narrow redshift ranges. Preprint at https://arxiv.org/abs/2505.20396 (2025).
47. Di Valentino, E. et al. Cosmology Intertwined III: $f\sigma_8$ and S_8. *Astropart. Phys.* **131**, 102604 (2021).
48. Perivolaropoulos, L. & Skara, F. Challenges for ΛCDM: an update. *N. Astron. Rev.* **95**, 101659 (2022).
49. Abdalla, E. et al. Cosmology intertwined: a review of the particle physics, astrophysics, and cosmology associated with the cosmological tensions and anomalies. *J. High Energy Astrophys.* **34**, 49–211 (2022).
50. Berryman, J. M. et al. Neutrino self-interactions: a white paper. *Phys. Dark Univ.* **42**, 101267 (2023).
51. Batell, B. et al. Dark sector studies with neutrino beams. Preprint at https://arxiv.org/abs/2207.06898 (2022).
52. Dvorkin, C., Blum, K. & Kamionkowski, M. Constraining dark matter–baryon scattering with linear cosmology. *Phys. Rev. D* **89**, 023519 (2014).
53. Boehm, C., Riazuelo, A., Hansen, S. H. & Schaeffer, R. Interacting dark matter disguised as warm dark matter. *Phys. Rev. D* **66**, 083505 (2002).

54. Cyr-Racine, F.-Y., de Putter, R., Raccanelli, A. & Sigurdson, K. Constraints on large-scale dark acoustic oscillations from cosmology. *Phys. Rev. D* **89**, 063517 (2014).
55. Bode, P., Ostriker, J. P. & Turok, N. Halo formation in warm dark matter models. *Astrophys. J.* **556**, 93–107 (2001).
56. Hu, W., Barkana, R. & Gruzinov, A. Cold and fuzzy dark matter. *Phys. Rev. Lett.* **85**, 1158–1161 (2000).
57. Amon, A. & Efstathiou, G. A non-linear solution to the S_8 tension? *Mon. Not. R. Astron. Soc.* **516**, 5355–5366 (2022).
58. Preston, C., Amon, A. & Efstathiou, G. A non-linear solution to the S8 tension—II. Analysis of DES Year 3 cosmic shear. *Mon. Not. R. Astron. Soc.* **525**, 5554–5564 (2023).
59. Di Valentino, E. et al. The CosmoVerse White Paper: addressing observational tensions in cosmology with systematics and fundamental physics. *Phys. Dark Univ.* **49**, 101965 (2025).
60. Dentler, M. et al. Fuzzy dark matter and the Dark Energy Survey Year 1 data. *Mon. Not. R. Astron. Soc.* **515**, 5646–5664 (2022).
61. Aghanim, N. et al. Planck 2018 results. V. CMB power spectra and likelihoods. *Astron. Astrophys.* **641**, A5 (2020).
62. Beutler, F. et al. The 6dF Galaxy Survey: baryon acoustic oscillations and the local Hubble constant. *Mon. Not. R. Astron. Soc.* **416**, 3017–3032 (2011).
63. Ross, A. J. et al. The clustering of the SDSS DR7 main Galaxy sample—I. A 4 per cent distance measure at $z = 0.15$. *Mon. Not. R. Astron. Soc.* **449**, 835–847 (2015).
64. Alam, S. et al. The clustering of galaxies in the completed SDSS-III Baryon Oscillation Spectroscopic Survey: cosmological analysis of the DR12 galaxy sample. *Mon. Not. R. Astron. Soc.* **470**, 2617–2652 (2017).
65. Gil-Marin, H. et al. The Completed SDSS-IV extended Baryon Oscillation Spectroscopic Survey: measurement of the BAO and growth rate of structure of the luminous red galaxy sample from the anisotropic power spectrum between redshifts 0.6 and 1.0. *Mon. Not. R. Astron. Soc.* **498**, 2492–2531 (2020).
66. Neveux, R. et al. The completed SDSS-IV extended Baryon Oscillation Spectroscopic Survey: BAO and RSD measurements from the anisotropic power spectrum of the quasar sample between redshift 0.8 and 2.2. *Mon. Not. R. Astron. Soc.* **499**, 210–229 (2020).
67. de Mattia, A. et al. The Completed SDSS-IV extended Baryon Oscillation Spectroscopic Survey: measurement of the BAO and growth rate of structure of the emission line galaxy sample from the anisotropic power spectrum between redshift 0.6 and 1.1. *Mon. Not. R. Astron. Soc.* **501**, 5616–5645 (2021).
68. du Mas des Bourboux, H. et al. The Completed SDSS-IV Extended Baryon Oscillation Spectroscopic Survey: baryon acoustic oscillations with Lyα forests. *Astrophys. J.* **901**, 153 (2020).
69. Alam, S. et al. Completed SDSS-IV extended Baryon Oscillation Spectroscopic Survey: cosmological implications from two decades of spectroscopic surveys at the Apache Point Observatory. *Phys. Rev. D* **103**, 083533 (2021).
70. Choi, S. K. et al. The Atacama Cosmology Telescope: a measurement of the Cosmic Microwave Background power spectra at 98 and 150 GHz. *J. Cosmol. Astropart. Phys.* **12**, 045 (2020).
71. Mead, A. et al. Accurate halo-model matter power spectra with dark energy, massive neutrinos and modified gravitational forces. *Mon. Not. R. Astron. Soc.* **459**, 1468–1488 (2016).
72. Madhavacheril, M. S. et al. The Atacama Cosmology Telescope: DR6 gravitational lensing map and cosmological parameters. *Astrophys. J.* **962**, 113 (2024).
73. Qu, F. J. et al. The Atacama Cosmology Telescope: a measurement of the DR6 CMB lensing power spectrum and its implications for structure growth. *Astrophys. J.* **962**, 112 (2024).
74. Carron, J., Mirmelstein, M. & Lewis, A. CMB lensing from Planck PR4 maps. *J. Cosmol. Astropart. Phys.* **09**, 039 (2022).
75. Fang, X., Eifler, T. & Krause, E. 2D-FFTLog: efficient computation of real space covariance matrices for galaxy clustering and weak lensing. *Mon. Not. R. Astron. Soc.* **497**, 2699–2714 (2020).
76. Krause, E. & Eifler, T. cosmolike—cosmological likelihood analyses for photometric galaxy surveys. *Mon. Not. R. Astron. Soc.* **470**, 2100–2112 (2017).
77. Hotelling, H. Analysis of a complex of statistical variables into principal components. *J. Educ. Psychol.* **24**, 417–441 (1933).
78. Hopkins, P. F. A new class of accurate, mesh-free hydrodynamic simulation methods. *Mon. Not. R. Astron. Soc.* **450**, 53–110 (2015).
79. Springel, V. The Cosmological simulation code GADGET-2. *Mon. Not. R. Astron. Soc.* **364**, 1105–1134 (2005).
80. Takahashi, R., Sato, M., Nishimichi, T., Taruya, A. & Oguri, M. Revising the Halofit model for the nonlinear matter power spectrum. *Astrophys. J.* **761**, 152 (2012).
81. Fang, X., Krause, E., Eifler, T. & MacCrann, N. Beyond Limber: efficient computation of angular power spectra for galaxy clustering and weak lensing. *J. Cosmol. Astropart. Phys.* **05**, 010 (2020).
82. Mandelbaum, R. et al. The LSST Dark Energy Science Collaboration (DESC) Science Requirements Document. Preprint at https://arxiv.org/abs/1809.01669 (2018).
83. Adamek, J., Durrer, R. & Kunz, M. Relativistic *N*-body simulations with massive neutrinos. *J. Cosmol. Astropart. Phys.* **11**, 004 (2017).
84. Bird, S., Viel, M. & Haehnelt, M. G. Massive neutrinos and the non-linear matter power spectrum. *Mon. Not. R. Astron. Soc.* **420**, 2551–2561 (2012).
85. Aghanim, N. et al. Planck 2018 results. VI. Cosmological parameters. *Astron. Astrophys.* **641**, A6 (2020).
86. Vagnozzi, S. et al. Unveiling *ν* secrets with cosmological data: neutrino masses and mass hierarchy. *Phys. Rev. D* **96**, 123503 (2017).
87. Jiang, J.-Q. et al. Neutrino cosmology after DESI: tightest mass upper limits, preference for the normal ordering, and tension with terrestrial observations. *J. Cosmol. Astropart. Phys.* **01**, 153 (2025).
88. Wang, D., Mena, O., Di Valentino, E. & Gariazzo, S. Updating neutrino mass constraints with background measurements. *Phys. Rev. D* **110**, 103536 (2024).
89. Adame, A. G. et al. DESI 2024 VI: cosmological constraints from the measurements of baryon acoustic oscillations. *J. Cosmol. Astropart. Phys.* **02**, 021 (2025).
90. Green, D. & Meyers, J. Cosmological preference for a negative neutrino mass. *Phys. Rev. D* **111**, 083507 (2025).
91. Elbers, W., Frenk, C. S., Jenkins, A., Li, B. & Pascoli, S. Negative neutrino masses as a mirage of dark energy. *Phys. Rev. D* **111**, 063534 (2025).
92. Herold, L., Ferreira, E. G. M. & Heinrich, L. Profile likelihoods in cosmology: when, why, and how illustrated with ΛCDM, massive neutrinos, and dark energy. *Phys. Rev. D* **111**, 083504 (2025).

Acknowledgements

This work is supported by the National Key Research and Development Program of China (grant no. 2022YFF0503304), the China Manned Space Program (grant no. CMS-CSST-2025-A03) and the Project for Young Scientists in Basic Research of the Chinese Academy of Sciences (grant no. YSBR-092). C.Z. is supported by the China Scholarship Council for 1-year study at SISSA. L.Z. is supported by the NAWA Ulam fellowship (grant no. BPN/ULM/2023/1/00107/U/00001). L.Z. and S.T. are supported by the National Science Centre, Poland (research grant no. 2021/42/E/ST2/00031). S.T. is also partially supported by Teaming for Excellence grant Astrocent Plus (GA: 101137080) funded by the European Union. E.D.V. acknowledges support from the Royal Society through a Royal Society Dorothy Hodgkin Research Fellowship. W.G. is supported by the Lancaster-Sheffield Consortium for Fundamental Physics under STFC

grant ST/X000621/1. This article is based upon work from the COST Action CA21136 'Addressing observational tensions in cosmology with systematics and fundamental physics' (CosmoVerse), supported by COST (European Cooperation in Science and Technology).

Author contributions

L.Z. conducted the cosmological simulations for this paper, with assistance from W.G. in their implementation. C.Z. was responsible for the *N*-body simulations, and S.T. wrote the first draft of the paper. E.D.V. and Y.-L.S.T. contributed to defining the project's scope and direction and provided insightful advice on interpreting the results. All authors participated in discussions and contributed to the preparation of the final draft.

Competing interests

The authors declare no competing interests.

Additional information

Supplementary information The online version contains supplementary material available at https://doi.org/10.1038/s41550-025-02733-1.

Correspondence and requests for materials should be addressed to Lei Zu, William Giarè, Chi Zhang, Eleonora Di Valentino, Yue-Lin Sming Tsai or Sebastian Trojanowski.

Peer review information *Nature Astronomy* thanks Antara Dey and the other, anonymous, reviewer(s) for their contribution to the peer review of this work.

Reprints and permissions information is available at www.nature.com/reprints.

Publisher's note Springer Nature remains neutral with regard to jurisdictional claims in published maps and institutional affiliations.

Open Access This article is licensed under a Creative Commons Attribution 4.0 International License, which permits use, sharing, adaptation, distribution and reproduction in any medium or format, as long as you give appropriate credit to the original author(s) and the source, provide a link to the Creative Commons licence, and indicate if changes were made. The images or other third party material in this article are included in the article's Creative Commons licence, unless indicated otherwise in a credit line to the material. If material is not included in the article's Creative Commons licence and your intended use is not permitted by statutory regulation or exceeds the permitted use, you will need to obtain permission directly from the copyright holder. To view a copy of this licence, visit http://creativecommons.org/licenses/by/4.0/.

© The Author(s) 2026